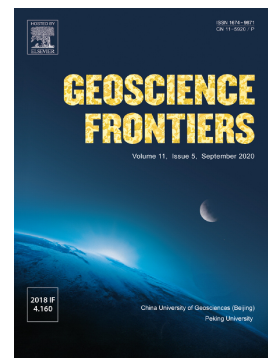


Journal Pre-proof

Particulate matter geochemistry of a highly industrialized region in the Caribbean: Basis for future toxicological studies

Luis F.O. Silva, Ismael L. Schneider, Paulo Artaxo, Yuleisy Núñez-Blanco, Diana Pinto, Érico M.M. Flores, Leandro Gómez-Plata, Omar Ramírez, Guilherme L. Dotto



PII: S1674-9871(20)30255-3
DOI: <https://doi.org/10.1016/j.gsf.2020.11.012>
Reference: GSF 1115

To appear in:

Received date: 16 September 2020
Revised date: 7 October 2020
Accepted date: 12 November 2020

Please cite this article as: L.F.O. Silva, I.L. Schneider, P. Artaxo, et al., Particulate matter geochemistry of a highly industrialized region in the Caribbean: Basis for future toxicological studies, (2020), <https://doi.org/10.1016/j.gsf.2020.11.012>

This is a PDF file of an article that has undergone enhancements after acceptance, such as the addition of a cover page and metadata, and formatting for readability, but it is not yet the definitive version of record. This version will undergo additional copyediting, typesetting and review before it is published in its final form, but we are providing this version to give early visibility of the article. Please note that, during the production process, errors may be discovered which could affect the content, and all legal disclaimers that apply to the journal pertain.

© 2020 Published by Elsevier.

**Particulate matter geochemistry of a highly industrialized region in the Caribbean:
basis for future toxicological studies**

Luis F.O. Silva ^{a,*} ; Ismael L. Schneider ^a , Paulo Artaxo ^{a,b} , Yuleisy Núñez-Blanco ^a ,
Diana Pinto^a , Érico M. M. Flores ^c , Leandro Gómez-Plata ^c , Omar Ramírez ^d , Guilherme
L. Dotto^e

^aDepartment of Civil and Environmental. Universidad de la Costa, CUC, Calle 58 # 55–66,
Barranquilla, Atlántico, Colombia

^bDepartment of Applied Physics, Institute of Physics - University of São Paulo, Brazil

^cDepartment of Chemistry, Universidade Federal de Santa Maria, RS, Brazil

^dUniversidad Militar Nueva Granada (UMNG), Faculty of Engineering, Environmental
Engineering, Km 2 Cajicá-Zipacquirá, Colombia

^eChemical Engineering Department, Federal University of Santa Maria - UFSM, 1000,
Roraima Avenue, 97105-900 Santa Maria, RS, Brazil.

***Corresponding author:**

Luis F. O. Silva: felipeqma@hotmail.com

Abstract

Air pollution has become an important issue, especially in Caribbean urban areas, and, particulate matter (PM) emitted by different natural and anthropogenic sources causes environmental and health issues. In this work, we studied the concentrations of PM₁₀ and PM_{2.5} sources in an industrial and port urban area in the Caribbean region of Colombia. PM samples were collected within 48-h periods between April and October 2018 by using a Partisol 2000i-D sampler. Elemental geochemical characterization was performed by X-ray fluorescence (XRF) analysis. Further, ionic species and black carbon (BC) were quantified by ion chromatography and reflectance spectroscopy, respectively. Using the Positive Matrix Factorization (PMF) receptor model, the contributions of PM sources were quantified. The average concentration of PM₁₀ was $46.6 \pm 16.2 \mu\text{g}/\text{m}^3$, with high concentrations of Cl and Ca. For PM_{2.5}, the average concentration was $12.0 \pm 3.2 \mu\text{g}/\text{m}^3$, and the most abundant components were C, S, and Cl. The receptor model identified five sources for PM₁₀ and PM_{2.5}. For both fractions, the contributions of marine sea spray, re-suspended soil, and vehicular traffic were observed. In addition, PM_{2.5} included two mixed sources were found to be fuel oil combustion with fertilizer industry emissions, and secondary aerosol sources with building construction emissions. Further, PM₁₀ was found to also include building construction emissions with re-suspended soil, and metallurgical industry emissions. These obtained geochemical atmospheric results are important for the implementation of strategies for the continuous improvement of the air quality of the Caribbean region.

Keywords: Urban Air Pollution; Particulate Matter; Geochemical Composition; Aerosol Source Apportionment; Receptor Models; PMF.

1. Introduction

The geochemical structure of air supports the existence of many organisms on Earth. Yet sensitive modifications in the atmospheric geochemistry conformation can lead to the heating of the world, depreciation of the O₃, and contaminated urban atmosphere. Air pollution in urban areas has become one of the major environmental problems, and it substantially impacts human health (Agudelo-Castañeda et al., 2016; WHO, 2018). The World Health Organization (WHO) estimates that 4.2 million people in both cities and rural areas die worldwide each year due to air pollution. Approximately 58%, 18%, and 6% of these deaths were associated with ischemic heart disease and stroke, chronic obstructive pulmonary disease and acute respiratory infections, and lung cancer, respectively (WHO, 2018). In Latin America and the Caribbean, air pollution has become a major concern owing to the increase in the concentrations of particulate matter and other air pollutants (Saldarriaga-Molina et al., 2004; Riojas-Rodríguez et al., 2016; Silva et al., 2020a). Among the atmospheric pollutants, one of the most hazardous is particulate matter (PM), which has various size fractions, being the finest the most dangerous. The important adverse results of ultra-fine particles have been confirmed in many previous studies and remained robust in the double-pollutant models adjusted for the mass concentrations of PM_{2.5} or even PM_{1.0}, including on mortality (Su et al., 2015), morbidity, pulmonary function, respiratory inflammation and oxidative stress, blood pressure (BP), and heart rate variability (HRV) (Chen et al., 2021), indicating the importance of UFPs control. Moreover, several previous studies have reported on the short-term health effects during substantial temporary improvements of ambient air quality or during indoor air quality interventions, focusing on

changes in health outcomes rather than on the changes in the relationships between health outcomes and air pollutants (Cui et al., 2018; Kubesch et al., 2015).

Particulate matter has diverse geochemical compositions depending on the natural and anthropogenic emission sources and its atmospheric processing (Duarte et al., 2019; Silva et al., 2020a,b). The only way to estimate and/or identify the contribution of each of these sources is via particle geochemical characterization. PM may include organic, mineral, and amorphous species, of which concentrations and composition vary spatially and temporally depending on the nature of the sources, so it is important to study PM composition to understand its dynamics and impact on the geochemistry environment (Arana and Artaxo, 2014; Cáceres et al., 2019). Some studies, especially, from developed countries, have identified the main PM sources and, further, by applying appropriate air quality management techniques, air pollution was reduced and population health improved (Wang et al., 2018).

However, in some developing countries (Ramírez et al., 2018) and Caribbean areas (Silva et al., 2020a), due to the lack of measurements, adequate aerosol source apportionment has not yet been achieved. Therefore, information on the geochemical characteristics of PM and identification of the emission sources are needed, specifically, the effect of meteorological variables, the concentration of pollutants in the atmospheric geochemistry, the duration of exposure to these concentrations, and the receptor characteristics are of high relevance. Multivariate receptor models are well-known tools for this type of scientific study. These have been used to identify and quantify the PM sources worldwide (Vallius et al., 2003; Scerri et al., 2016; Farahmandkia et al., 2017; Bhuyan et al., 2018; Wu et al., 2018; Saraga et al., 2019;). Positive Matrix Factorization (PMF) model is a factor-based receptor model that uses the weighted least-squares fit of the

observation data for the identification of the optimal results for the factors/sources (Police et al., 2018). The PMF model is used as a tool to identify sources of atmospheric PM and quantify their respective contributions, especially in highly polluted industrialized urban areas (Reff et al., 2007; Brito et al., 2013; Salvo et al., 2017; Cesari et al., 2018; Morera-Gómez et al., 2018; Saraga et al., 2019). These data must be reliable, valid, and up-to-date to acquire information about the characteristics of the atmosphere, which will enable not only effective scientific decision making but also facilitate long-term early alerts and the development of new environmental policies that will help to mitigate and control pollution (Song et al., 2016).

In recent years, rapid industrial development, especially in relation to fertilizer factories; cement, iron ore, and steel industries; waste incineration; civil works projects; and increased vehicular traffic in the Caribbean city of Barranquilla, Colombia, is affecting the air quality of the region (Castillo-Ramírez et al., 2018; Silva et al., 2020a). Steel industries are a major environmental pollution source as they release numerous contaminants as particulate matter (PM), gas and vapour. Most PM wastes from these industries contain iron, carbon powder, and silicon (Yan et al., 2010), and minor elements such as Pb, Al, Zn, Mn, Cr, Cd, Cu, Ni, Ti, V, and other trace hazardous elements. The legislation for monitoring and controlling atmospheric contamination is usually based on the definition that PM is a complex mixture of solid particles, containing both organic and inorganic substances, suspended as aerosols in air together with liquid droplets. PM fractions having a diameter of 10 μm or less (PM₁₀) are recognized as potentially harmful to humans (WHO, 2018). In this context, for industrialized urban areas with such a complex environment, geochemical studies are needed to determine the pollutants and the contribution of each source, with a focus on the PM fractions PM₁₀ and PM_{2.5}. This

information will allow the generation of a baseline for the air quality of the Caribbean region, thus enabling authorities to establish criteria for the mitigation and control of air pollution in the region.

The multiple PM sizes released in the atmosphere during smelting vary according to the alloys produced, the composition of the original ore, and the industrial process applied, in addition to the high melting temperature and/or the additives used in the process (Badillo-Castañeda et al., 2015). The PM released in the smoke can be coarse, fine, ultrafine, and nanoparticles (the latter NPs with at least in one dimension ≤ 100 nm), which have a high potential to reach the respiratory system (Arick et al., 2015). Furthermore, metallic NPs have been widely used in steel production to improve weld strength and this may increase their release to the environment (Kumar et al., 2018). NPs are continuously used in numerous industries, including the steel ones; however, environmental regulations have not yet been established, as their action is not fully understood.

This study reinforces the need for more studies on Caribbean areas because there have been few investigations focused on these environments that have unique atmospheric geodynamics; in particular, the dispersion processes of atmospheric PM, as well as the contribution of significant natural sources, specifically marine aerosols and soil re-suspension, in these areas, are more significant than those in other industrialized urban Caribbean areas.

2. Materials and Methods

2.1. Selected study Area

According to the reviews conducted, the atmospheric geochemistry of the Caribbean area has never been evaluated in terms of source estimates. Therefore, this study will serve

to collaborate with other industrialized and urban Caribbean regions. The city of Barranquilla ($10^{\circ}59'16''\text{N}$, $74^{\circ}47'20''\text{W}$) is the capital of the department of Atlántico in North Colombia and is located on the Atlantic Caribbean coast at an elevation of 18 m.a.s.l. It has an area of 154 km^2 and a population of approximately 1.2 million (Alcaldía de Barranquilla, 2020). The climate of Barranquilla is classified as tropical dry and is characterized by a wet period from April to November and a dry one from December to March. The average annual rainfall and temperature are 767 mm and 27°C , respectively, and the wind direction from the northeast is constant (CIOH, 2007).

Barranquilla is officially referred to as a special, industrial, and port district. It is a coastal city with several industries, especially for producing beverages and food and manufacturing of metal products and geochemical substances and/or products. However, in addition to the economic benefits resulting from these industrial activities, they contribute to the deterioration of air quality in the urban area owing to the increase in atmospheric-pollutant concentrations (Vélez-Pereira and Vergara-Vasquez, 2013).

In this study, the sampling site for atmospheric PM (PM_{10} and $\text{PM}_{2.5}$) was located on the roof of the Universidad de la Costa ($10^{\circ}59'41.85''\text{N}$, $74^{\circ}47'27.65''\text{W}$) (Fig. 1). This monitoring site was selected because it is downwind from multiple sources of local pollution, including vehicular traffic, industrial emissions, and biomass burning in the Salamanca Island Park, a nature reserve located near the study area. These are representative sources that significantly increase the levels of atmospheric pollutants in the study area (Fig. 2).

2.2. PM sampling

PM₁₀ and PM_{2.5} aerosol sampling was carried out between April and October 2018. To define the optimal sampling time, preliminary tests were carried out by varying the sampling time from 24 h to 48 h, to determine the optimal sampling time. The tests showed that optimal sampling was achieved with 48-h sampling for each filter, and a total of 83 samples were obtained during this period. A Partisol Dichotomous 2000i-D sampler (Thermo Fisher Scientific) was used to collect PM using 47-mm-diameter PTFE filters. The sampler has a virtual impactor and can simultaneously collect the fine (PM_{2.5}) and coarse (PM_{2.5-10}) mode aerosol fractions. The PM₁₀ concentrations correspond to the sum of the concentrations of the two fractions. This equipment operates with a PM₁₀ inlet and a total flow rate of 16.7 L/min. Internally, the flow is separated using a virtual impactor into two with a 15 L/min flow rate for the fine particles and 1.67 L/min for the coarse fraction.

The PM₁₀ and PM_{2.5} concentration were determined gravimetrically with a Sartorius microbalance. Before weighing, all filters were conditioned in a desiccator and then weighed in a room with controlled temperature and relative humidity conditions (25 ±2 °C and 40% ±5%, respectively). A deionizer was used to neutralize the electrostatic charges of the filters (Taiwo, 2016). The weighing was repeated for filters with and without aerosol collection until three replicates achieved a weight difference of less than <10 µg. Careful measurements with a blank control helped in achieving good accuracy and low standard deviation.

Meteorological parameters such as the precipitation, wind speed and direction, temperature, relative humidity, and solar radiation were measured with a Davis Vantage Pro2 meteorological station. The meteorological data were collected every 5 min, and after each filter collection, the values were averaged for the 48 h of sampling.

2.3. Geochemical characterization

The aerosol samples were geochemically characterized to determine the levels of the major and trace elements, soluble ions (for $PM_{2.5}$), and the black carbon (BC) concentrations associated with PM_{10} and $PM_{2.5}$. X-Ray fluorescence (XRF) analysis was performed in the laboratory of the Companhia Ambiental do Estado de São Paulo (CETESB), Brazil, with a PANalytica Epsilon 5 spectrometer. The calibration and optimization methodology of the instrument were the same as those developed by Arana and Artaxo (2014). The measurement time for light elements (Na to K) was 600 s and that for heavy elements (Ca to Pb) was 300 s, corresponding approximately to 1 h of measurement for each sample (Arana and Artaxo, 2014; Contini et al., 2016; Scerri et al., 2016). The detection limits (DL) for each element are within a range of 0.001–0.015 $\mu\text{g}/\text{m}^3$.

After XRF analysis, the concentrations of cations and anions for $PM_{2.5}$ were obtained using ion chromatography. The concentrations of Ca^{2+} , K^+ , Mg^{2+} , and Na^+ (in the soluble fraction) were determined with an inductively coupled plasma optical emission spectrometer (ICP-OES; Optima model 4300 DV, Perkin Elmer) equipped with a GemCone[®] nebulizer and a cyclonic spray chamber. Argon (99.996%; Air Products, Brazil) was used for the generation of plasma, nebulization, and auxiliary gas. In addition, the concentrations of Cl^- , NO_3^- , and SO_4^{2-} were determined by ion chromatography with a Metrohm IC model 850 professional and a conductivity detector. These analyses were performed in the Chemistry Department of the Universidade Federal de Santa Maria, Brazil (Morera-Gómez et al., 2018; Querol et al., 2002).

The concentrations of black carbon (BC) were determined by using a reflectance technique (optical absorption). The measurements are made with a diffuse white light reflectometer from Diffusion Systems. The calibration procedure used is the same that

established by Santos Junior (2009). These analyses were performed in the Universidad de la Costa, Colombia.

2.4. Aerosol source apportionment

The contribution of each of the PM sources was estimated using the PMF receptor model (Paatero and Tapper, 1994; Tasić et al., 2009; Morera-Gómez et al., 2018; Ramírez et al., 2018; Saraga et al., 2019). The objective is to identify the number of factors/sources, their chemical profiles, and the mass associated with each source that contributed to the measured PM concentrations (Cesari et al., 2018). Knowledge about the source profiles is not needed to use the PMF model, and it is quite easy to use (Zhong et al., 2018); in addition, its effectiveness has been demonstrated in many studies on urban areas worldwide (Gu et al., 2014; Contini et al., 2016; Gao et al., 2016).

The PMF model version 5.0, developed by the US EPA (USEPA, 2014), was used in this study. The fundamental principle in this receptor model is that mass conservation can be assumed, and a mass balance analysis can be used for the identification and apportionment of sources of airborne PM (Hopke, 2003):

$$x_{ij} = \sum_{k=1}^p g_{ik} f_{jk} + \sigma_{ij} \quad i = 1, 2, \dots, m \quad j = 1, 2, \dots, n \quad (1)$$

where x_{ij} is the concentration of the j^{th} species measured in the i^{th} sample, g_{ik} is the contribution of the k^{th} source to the i^{th} sample, f_{jk} is the concentration of the j^{th} species in the k^{th} source, and σ_{ij} is the residual associated with the concentration of the j^{th} species

measured in the i^{th} sample. The objective of PMF modeling is to minimize the sum of the squares of the residuals weighted with the estimated uncertainties.

Uncertainties were calculated according to the DL and the proximity of the concentrations of each element to this DL. When the concentrations were equal or close to the DL, the uncertainty was greater (250%), and when the concentrations were higher, the uncertainty was lower (5%). When an element could not be determined (i.e., concentrations below the DL), it was considered with an uncertainty of 400%. Also, each evaluated element was classified as "Strong" (when the signal-to-noise ratio (SN) was >1.0), "Weak" (when $0.2 < \text{SN} < 1.0$), or "Bad" (when $\text{SN} < 0.2$) (Viana et al., 2006; Vargas et al., 2011; Ramírez et al., 2018). For the fine and coarse fractions, 21 and 16 species, respectively, were selected as the strong species. The proximity of Q_{robust} and Q_{theory} values was used as a criterion to select the best fit of the model corresponding to the number of factors used (from four to six factors). The best solution was obtained using five factors for each PM fraction, which have a reasonable interpretation since the residues were distributed symmetrically for almost all the elements, which means that the model can reasonably adapt to each chemical species (Cesari et al., 2018). In addition, considering fewer factors resulted in many mixed sources, and in contrast, a higher number of factors resulted in sources with few associated elements.

The reconstructed mass or mass closure calculations for PM_{10} and $\text{PM}_{2.5}$ corresponded to the arithmetic sum of the average concentrations of each chemical component, which in this study included the following: BC, the major and trace elements determined by analyzing 25 possible elements (Mg, Al, Si, P, S, Cl, K, Ca, Ti, V, Cr, Mn, Fe, Ni, Cu, Zn, Ga, As, Cd, Sn, Sb, Pb, Sr, Rb), and soluble ions only for the fine fraction ($\text{PM}_{2.5}$). The concentrations

of Cr, Ga, As, Se, Cd, Sn, Sb, Sr, Rb, Rh, Pd, and Pt were in general below the DL, and therefore, these elements were not considered in the statistical analyses.

2.5. Statistical analysis

To analyze the behavior of the PM and chemical concentrations and meteorological parameters data, a normality test, i.e., the Kolmogorov–Smirnov statistical test, was carried out with a confidence level significance of 95% and a p-value of 0.05. In this way, the behavior of the data allowed that the non-parametric test should be used, since it better adjusts to a non-Gaussian data distribution. Also, Spearman's correlation coefficient was used, since it can be used for non-normal data distribution (Delicado, 2008). In addition, a correlation matrix was employed to evaluate the strength of the relationship between the variables and thus to validate the chemical and geochemical analysis results.

3. Results and discussion

3.1. Mass and chemical concentration of PM₁₀ and PM_{2.5}

The results of descriptive analysis for the 88 samples evaluated are shown in Table 1, which presents the arithmetic average, minimum, maximum, and standard deviation of the concentrations of the PM and each chemical element evaluated. From April to October 2018, the average concentration of PM_{2.5} was $12.0 \pm 3.2 \mu\text{g}/\text{m}^3$, and that of PM₁₀ was $46.6 \pm 16.2 \mu\text{g}/\text{m}^3$. A comparison with the results of IDEAM (2018), who performed similar measurements in other Colombian cities, for aerosol compositions in Bogotá and Medellín, shows that the concentrations in Barranquilla are lower. At present, each country has applied specific regulations for outdoor and indoor environments, with an aim to minimize and prevent health problems. The atmospheric PM limits recommended by the World

Health Organization (WHO, 2018) has a maximum of $50 \mu\text{g}/\text{m}^3$ in 24 h for PM_{10} but, based on an annual monitoring, the daily mean cannot exceed $20 \mu\text{g m}^{-3}$ in the same period. For the fine particulates ($\text{PM}_{2.5}$), the maximum recommended value reach $25 \mu\text{g}/\text{m}^3$ in 24 h, with a daily mean of $10 \mu\text{g}/\text{m}^3$ in the same period (Bourdrel et al., 2017). The regulatory analysis of air quality usually quantifies PM_{10} and $\text{PM}_{2.5}$ filtered from air over 24 h and captured in a membrane with appropriate pore size; the difference between the membrane mass before and after the sampling process is considered as the total amount of PM in the air (Cereceda-Balic et al., 2017).

Upon evaluating the relationship between the concentrations of PM_{10} and $\text{PM}_{2.5}$, it is observed that the fine fraction corresponds, on average, to 26% of the PM_{10} concentrations. When comparing this percentage with the values obtained in other urban cities in Latin America, it is observed that the percentage in Barranquilla is lower than that in Córdoba, Argentina; Belén, Costa Rica; and Mexico City, Mexico (Table 2). This is attributed to the characteristics of the study area which, in addition to being a coastal area, is strongly influenced by the trade winds from the northeast (from the Caribbean Sea), which facilitate the dispersion of the fine fraction. Further, Barranquilla has a flat urban area, which contributes to the dispersion of fine particles due to their small mass. The latter is because the atmospheric PM consists of chronic and diffuse contamination in which one source may disperse particles to a large area (Tiwarý and Williams, 2018). During the rainy season the atmospheric PM can be dispersed and dissociated in the nanoscale and percolate into the subsoil and affect groundwater until it reaches rivers, lakes, estuaries, and the ocean. Therefore, to exclude the possibility of overexposure to nanoscale particles in areas in which the atmospheric PM can contaminate hydrological resources, additional tests should be incorporated in environmental analyses related to atmospheric PM dispersion in the

aqueous system and including size measurements, for example, NanoSight for Nanoparticle Screening (NTA). Thus, the effects of atmospheric particulate emissions for aquatic biota can be understood more accurately with this newly-observed process.

The variations in the PM_{10} and $PM_{2.5}$ concentrations for each sample (corresponding to a 48-h sampling period) are shown in Fig. 3. The maximum concentration of $PM_{2.5}$ was $20.1 \mu\text{g}/\text{m}^3$ on June 7, 2018. For PM_{10} , the highest concentration of $109.2 \mu\text{g}/\text{m}^3$ was registered on October 3, 2018. These high results are associated with activities that were carried out in the city during the sampling period, such as building construction close to the site, stream channeling, increase in vehicular traffic and emissions from fertilizer production and metallurgy industry close to the study area. These increases in the concentrations of PM were also associated with the same sources in a report by the local environmental authority (Castillo-Ramírez et al., 2018). The behavior of atmospheric PM is strongly affected by meteorological variables and urban dynamics (Ramírez et al., 2018). In particular, the constant winds blowing from the Atlantic Ocean (Caribbean Sea) into the country have a substantial impact. The windiest period extends from November to May with average speeds of 4.5 m/s , while in the other months, wind speeds are lower than 3 m/s (CIOH, 2007). During the day, the highest speeds are seen from noon up to the early hours of the next day (Palomino, 2016).

According to the results of the chemical characterization of the PM (Table 1), the most abundant species (in terms of the mass) was BC for both the $PM_{2.5}$ ($1.14 \pm 0.59 \mu\text{g}/\text{m}^3$) and PM_{10} ($2.13 \pm 1.12 \mu\text{g}/\text{m}^3$) fractions, an element emitted mainly from diesel vehicles or from burning biomass (Kholod & Evans, 2016). Sulfur was present in a high proportion in the fine fraction ($0.81 \pm 0.17 \mu\text{g}/\text{m}^3$). The presence of sulfur-rich particles, in general, is associated with fossil fuel combustion processes (WHO, 2005), and sulfur can react in the

atmosphere to form secondary aerosols, resulting in an increase in sulfate concentrations (Ordóñez-Aquino and Sánchez-Ccoyllo, 2017). Further, high concentrations of chlorine were observed in both $PM_{2.5}$ ($0.74 \pm 0.59 \mu\text{g}/\text{m}^3$) and PM_{10} ($4.03 \pm 1.99 \mu\text{g}/\text{m}^3$), due to the proximity of the study area to the ocean, and this is associated with marine aerosols (Argumedo & Castillo, 2016; Scerri et al., 2016). Likewise, the concentrations of magnesium ($0.21 \pm 0.10 \mu\text{g}/\text{m}^3$), aluminum ($0.37 \pm 0.34 \mu\text{g}/\text{m}^3$), silicon ($0.58 \pm 0.51 \mu\text{g}/\text{m}^3$), calcium ($0.19 \pm 0.06 \mu\text{g}/\text{m}^3$), and iron ($0.20 \pm 0.16 \mu\text{g}/\text{m}^3$) in $PM_{2.5}$ were high and are associated with soil resuspension (Aldabe et al., 2011).

On the other hand, for PM_{10} , calcium ($1.70 \pm 0.47 \mu\text{g}/\text{m}^3$) is present in the atmospheric dust in the form of carbonates and is significantly involved in the neutralization of the atmospheric acids (Argumedo and Castillo, 2016). However, chlorine reacts with calcium or aluminum to form chlorides (Ordóñez-Aquino and Sánchez-Ccoyllo, 2017). Further, in both fractions, similar concentrations of BC, Mg, P, Cu, and Zn were observed. The following sections detail the contributions of the different elements.

3.2. PM_{10} and $PM_{2.5}$ mass closure calculations

The chemical composition of the particles determines their toxicological potential and behavior in the atmosphere, and it is a very important factor for assessing the contribution of different sources, especially in the development of strategies to control and reduce air pollution (Rojano et al., 2014; Park et al., 2018;). Fig. 4 shows the mass closure results for PM_{10} and $PM_{2.5}$. The sum of the masses of the measured compounds represents 28% and 60% of the PM_{10} and $PM_{2.5}$ fractions.

For the $PM_{2.5}$ fraction, the average contributions of the evaluated elements in this investigation were as follows: the amounts of the major elements—Mg, Fe, Al, Si, P, S, Cl,

K, Ca, and Ti—correspond to 26% of the total mass, while those of the trace elements—V, Mn, Ni, Cu, Zn, and Pb—and BC correspond to 2% and 9%, respectively. Further, soluble ions— Mg^{2+} , Ca^{2+} , Cl^- , NO_3^- , and SO_4^{2-} —corresponded to 23% of the $\text{PM}_{2.5}$ mass. This last group may be associated mainly with secondary inorganic aerosol species (Cesari et al., 2018). In the atmosphere, chemical reactions can occur to form secondary aerosols, generating an increase in sulfate concentrations (Ordóñez-Aquino & Sánchez-Ccoyllo, 2017; Tomasi et al., 2017). The results of this study agreed well with those of previous studies, as can be observed in Table 2, which also shows the greatest contributions associated with sulfates and nitrates (Murillo et al., 2013; Wang et al., 2006). The most abundant species in terms of the mass in the fine fraction ($\text{PM}_{2.5}$) is BC ($1.14 \pm 0.59 \mu\text{g}/\text{m}^3$), which agrees with the results of Arana and Artaxo (2014). The nonmetallic sulfur ($0.81 \pm 0.17 \mu\text{g}/\text{m}^3$) and chlorine ($0.74 \pm 0.59 \mu\text{g}/\text{m}^3$) were also abundant in this fraction. The presence of sulfur-rich particles, in general, is associated with fossil fuel combustion processes (WHO, 2005). Further, due to the proximity of the study area to the ocean, chlorine is associated with marine aerosols (Scerri et al., 2016). Likewise, significant magnesium ($0.21 \pm 0.10 \mu\text{g}/\text{m}^3$), aluminum ($0.37 \pm 0.34 \mu\text{g}/\text{m}^3$), silicon ($0.58 \pm 0.51 \mu\text{g}/\text{m}^3$), calcium ($0.19 \pm 0.06 \mu\text{g}/\text{m}^3$), and iron ($0.20 \pm 0.16 \mu\text{g}/\text{m}^3$) contents were observed in the $\text{PM}_{2.5}$ fraction, and these elements were associated with soil resuspension (Aldabe et al., 2011). The remaining 40% of the $\text{PM}_{2.5}$ mass probably corresponds to organic matter, elemental and organic carbon, and organic species that could not be traced in this investigation (Gu et al., 2014).

The PM_{10} mass closure calculations presented a BC content of 4%, and the content of the major elements (Mg, Fe, Al, Si, P, S, Cl, K, Ca, and Ti) was 22%—i.e., the most abundant group in this fraction (Yin & Harrison, 2008). The trace elements (V, Mn, Ni, Cu,

Zn, and Pb) accounted for only 2% for the PM₁₀ concentration. Further, the high resuspended dust content was evident from the amounts of soil dust tracers such as Al, Ca, Fe, Si, and Ti (Lu et al., 2018). In addition, for the coarse fraction, the most abundant species were chlorine ($4.03 \pm 1.99 \mu\text{g}/\text{m}^3$), the main tracer of marine aerosols (Contini et al., 2010), BC ($2.13 \pm 1.12 \mu\text{g}/\text{m}^3$), which in its recalcitrant form is a fundamental constituent of soil organic matter (Archanjo et al., 2014), and calcium ($1.70 \pm 0.47 \mu\text{g}/\text{m}^3$), which is present in atmospheric dust in the form of carbonates and acts in the neutralization of atmospheric acids (Argumedo and Castillo, 2016). Moreover, in both fractions, BC, Mg, P, Cu, and Zn contents were similar.

Further, on average, 72% of the PM₁₀ mass, i.e., $52.5 \mu\text{g}/\text{m}^3$ was composed of unknown constituents, whereas for the fine fraction, the unknown constituents corresponded to $4.79 \mu\text{g}/\text{m}^3$ or 40% of the PM_{2.5} mass; these constituents are believed to be particles of organic matter and minerals rich in organic matter and elemental carbon (Terzi et al., 2010; Jain et al., 2018). Further, water-bound components in PM have been estimated to correspond to 20%–35% of the total PM mass (Tsyro, 2005). The PM₁₀ fraction is generally formed via the mechanical disintegration of materials or the resuspension of particles due to road traffic, the so-called resuspended road dust (Amato et al., 2016). It has been established that these particles, in general, are made up of seven chemical components or species: geological material, ammonium sulfates, ammonium nitrates, organic matter, elemental carbon, salts, and trace elements (Canales-Rodríguez et al., 2014). Further, the fine particles (PM_{2.5}) are generally composed of ammonium nitrates, sulfates, BC, and secondary organic carbon (Ordóñez-Aquino and Sánchez-Ccoyllo, 2017).

3.3. Source apportionment

PM primary or secondary particles, especially in urban areas, originate from the vehicular traffic, energy-generation plants, industrial sources, natural sources, and the secondary aerosols formed by gas-to-particle conversion (Schneider et al., 2015). In this study, PMF was used to determine the PM emission sources, and four to six factors were analyzed to obtain the optimal result. The values of Q generated by PMF (robust and theoretical), the chemical profiles, and the relationship between modeled and measured concentrations of each factor were evaluated. The best solutions were found for five factors for both PM_{10} and $PM_{2.5}$ fractions and are presented in Figs. 5 and 6. The blue columns and the red squares represent the mass contribution of the species to the factor ($\mu\text{g}/\text{m}^3$), and the percentage of species in the factor, respectively. Further, in Fig. 7, the contribution factor for each estimated source is presented. 10^1 10^{-1} 10^{-2} 10^{-3} 10^{-4} 10^0

For $PM_{2.5}$, the PMF receptor model gave the following factors:

- F1 (Fuel oil combustion and fertilizer industries): Due to the variety of elements present, this factor was considered to represent mixed sources, characterized by high contributions of S, V, Ni, Pb, K^+ , P, and SO_4^{2-} . The elements, Ni, V, and Cu, are associated with fuel oil burning (Soleimani et al., 2018), and Ni and V, in particular, are indicators of heavy oil combustion in cargo ships—that is, associated with port operations (Wang et al., 2018)—or in industrial boilers (Vallius et al., 2003; Police et al., 2018). On the other hand, K is a tracer of various sources, including biomass burning, fertilizer industry emissions, or soil dust. However, during the sampling period considered in this study, no biomass burning event was observed upwind of the study area, and therefore, K was not associated with this source. Therefore, Ca, P, K^+ , and SO_4^{2-} were associated with fertilizer production (Ordóñez-Aquino and Sánchez-Ccoyllo, 2017). In Barranquilla, there are around 40 companies that produce, pack,

and distribute fertilizers. This factor corresponds to 36.0% ($4.05 \mu\text{g}/\text{m}^3$) of the $\text{PM}_{2.5}$ content.

- F2 (Marine aerosols): This factor represents 17.0% ($1.92 \mu\text{g}/\text{m}^3$) of the $\text{PM}_{2.5}$ content. The largest contributions were from Mg, Cl, Na^+ , K^+ , Mg^{2+} , and Cl^- , so it is associated with marine aerosols. Marine aerosols are formed by the effect of winds on the ocean surface, which generates emissions of sea salt and inorganic ions (Bhuyan et al., 2018; Police et al., 2018; Vengoechea et al., 2018).
- F3 (Secondary sources and construction works): In the presence of Ca^{2+} , NO_3^- , and SO_4^{2-} , this factor was also considered to represent a mixed source. Several studies associated the presence of NO_3^- and SO_4^{2-} with the processes of conversion of gaseous precursors NO_x and SO_2 to particles (Tao et al., 2014; Song et al., 2016; Perrone et al., 2018; Zhou et al., 2018). On the other hand, Ca^{2+} is a marker for limestone, so sources likely include fugitive emissions from construction and demolition work and other activities related to the use of limestone in the construction industry (Wang et al., 2006; Contini et al., 2016; Scerri et al., 2016). This factor corresponded to 11.3% ($1.32 \mu\text{g}/\text{m}^3$) of the $\text{PM}_{2.5}$ concentration.
- F4 (Vehicular traffic): In the presence of BC, Mn, Zn, Cu, and Pb, this source represented 12.9% ($1.45 \mu\text{g}/\text{m}^3$) of the $\text{PM}_{2.5}$ concentration. Further, the BC content is consistent with emissions mainly from diesel vehicle emissions (Kholod and Evans, 2016; Police et al., 2018), and the Mn content is associated with gasoline vehicle exhaust, as it is used to improve the combustion processes (Cheung et al., 2010). Elements such as Zn, Mn, Cu, and Ni have been related to vehicle exhaust emissions, mainly associated with the compositions of the fuel and oil lubricants, and Cu, Pb, and

Zn in the PM originate due to tire wear and abrasion of vehicle brakes (Jaiprakash and Habib, 2017; Liu et al., 2018).

- F5 (Resuspended soil): This source contributed to 22.3% ($2.51 \mu\text{g}/\text{m}^3$) of the $\text{PM}_{2.5}$ concentration. It was characterized by the presence of Al, Si, K, Ti, Mn, and Ca. The materials in the crust contribute to the atmospheric aerosol mass, and soil particles can be carried by the wind, especially when the soil is mechanically altered or during dry periods (Putaud et al., 2010; Police et al., 2018; Zhou et al., 2018).

For PM_{10} , the PMF receptor model gave the following factors.

- F1 (Metallurgical industry): This source contributed to 11.3% ($5.23 \mu\text{g}/\text{m}^3$) of the PM_{10} concentration. This factor was associated to Zn, S, Cu, and Cr, which are indicative of metallurgy emissions, and, in general, are associated with coarse particles (Xue et al., 2018; Zhong et al., 2018).
- F2 (Resuspended soil): This source has a contribution of 20.4% ($9.48 \mu\text{g}/\text{m}^3$) to the PM_{10} concentration, and it predominantly presents Al, Si, Mg, Ti, K, and Fe. This source is compatible with an increase in the concentration of species mainly related to the earth's crust (Cecari et al., 2018). In addition, resuspension of soil and arid soil particles are the main sources of these elements in PM_{10} (Contini et al., 2016).
- F3 (Resuspended soil and construction work): The contribution of this factor to the PM_{10} concentration was 34.2% ($15.88 \mu\text{g}/\text{m}^3$). The elements present in greater proportions were Ti, Mn, and Fe that may originate from the limestone used in civil works or present in geological material (Contini et al., 2016). Ti and Mn can be derived from iron or steel used in civil works (Liu et al., 2016).

- F4 (Vehicular traffic): This source is associated with BC, Ca, Zn, and to a lesser extent with Ni, P, and Cu, contributing 4.3% ($1.98 \mu\text{g}/\text{m}^3$) to the PM_{10} concentration. Cu and Zn are emitted by the wear of vehicle brakes and tires (Farahmandkia et al., 2017), and Zn can also be emitted in the exhaust from the combustion of fuel and/or lubricating oil; further, BC is formed from the incomplete combustion of fossil fuels (Tasić et al., 2009; Maldonado-Arízaga, 2012; Hao et al., 2018).
- F5 (Marine spray): This source, with a predominant concentration of Cl, contributed to 29.8% ($13.80 \mu\text{g}/\text{m}^3$) of the PM_{10} concentration. The city of Barranquilla is located at a distance of 7.5 km from the Caribbean Sea and the constant winds between the northeastern and eastern directions bring marine aerosols generated by the action of winds on the ocean surface.

In Table 3, Spearman's correlation matrix between the PM concentrations and the meteorological parameters are presented. The correlations corresponding to PM_{10} and $\text{PM}_{2.5}$ are presented in red and black, respectively. As can be seen, PM_{10} and $\text{PM}_{2.5}$ have a highly significant correlation ($\rho = 0.890$), indicating similar variability. This information was also confirmed through the receptor model presented above, so the two fractions presented similar sources with varying contribution percentages. Similar results were observed in other studies (López et al., 2011; Murillo et al., 2013; Arana and Artaxo, 2014; Li et al., 2016; Yao et al., 2016).

Table 3 shows the influence of meteorological variables—solar radiation ($\rho = 0.317$) and wind speed ($\rho = 0.280$)—on the concentrations of $\text{PM}_{2.5}$. Dry conditions are conducive to the resuspension of fine particles (Pedro et al., 2011). The influence of the meteorological parameters (Table 3) on PM_{10} is similar to that observed for $\text{PM}_{2.5}$, with the

exception of precipitation: in the case of the PM_{10} fraction, it presents a significant influence ($\rho = -0.316$). This inverse correlation between precipitation and PM_{10} is related to the rain removal process (Pillai et al., 2002; Blanco-Becerra et al., 2015). In general, all the results obtained in this study can be used for the development of plans for air quality management in the region, since it was possible to highlight the main PM sources on which local authorities can focus the control and mitigation measures. Thus, despite the aerial animal and human exposure to atmospheric pollution, a second contamination pathway should be evaluated when regulating atmospheric PM emissions, considering that the aquatic system can be the direct or indirect receptor of larger and smaller PM. Moreover, nanoparticles present in the PM can be incorporated into aquatic biota and further transferred to humans by food consumption (Souza et al., 2019). Hence, more research linking atmospheric pollution, and aquatic pollution is necessary since only few studies have focused on this contamination pathway. Most environmental regulations remain unclear about these issues, which are causing deleterious effects to several organisms and human health.

The multiple patterns of heart rate variability indices changed with $PM_{2.5}$ and UFPs at low $PM_{2.5}$ concentrations, which was consistent with the results of previous authors (Chen et al., 2021). Studies in Europe and Canada showed that significant changes in heart rate variability indices with varying $PM_{2.5}$ and UFPs occurred at lag 0- and 1-day (with peak values at lag 2-day), respectively; even though $PM_{2.5}$ concentrations were much lower than those in China, the UFP concentrations were similar (Weichenthal et al., 2014; Peters et al., 2015). The present work contributed information on geochemical of $PM_{2.5}$ concentrations. To our best knowledge, it is the first study to report the different chemical compositions at different $PM_{2.5}$ concentrations in Caribbean area. Compared with $PM_{2.5}$, the small sizes

allowed UFPs to penetrate deeper and evade the clearance from the respiratory tract (Li et al., 2016). The different behaviors of PM_{10} and $PM_{2.5}$ in the human respiratory tract may contribute to the differences in associations with cardiovascular indices.

4. Conclusion

In this study, the concentrations of the atmospheric particulate matter (PM_{10} and $PM_{2.5}$) and the chemical elements associated with each fraction were evaluated to identify the contributions of the main emission sources. The results showed that the fine fraction corresponds to just 26% of the PM_{10} mass concentration, a low ratio for urban areas. This can be attributed mainly to the processes of dispersion and dilution of $PM_{2.5}$, which depend on the wind speed and direction, and also coupled with the proximity of the study area to the Caribbean Sea and the topography of the region. The mass closure calculation results indicated that 28% and 60% of the PM_{10} and $PM_{2.5}$ mass was identified by PMF. Therefore, future research should consider more compounds and/or elements not evaluated in this study. It was also observed that for both fractions, the BC, Mg, P, Cu, and Zn contents are similar. The predominant sources for PM_{10} were civil works and resuspended soil with a contribution of 34.2% and marine spray with a contribution of 29.8%. For the fine fraction, the main sources were fuel oil combustion and fertilizer industry emissions with a contribution of 36%, followed by resuspended soil with 22.3% contribution. These results are attributed to the fact that in the city of Barranquilla, during the sampling period, civil construction of sports complexes and stream channeling were underway, in addition to an increase in the vehicle fleet, production of fertilizers, and metallurgy work, as a result of the regional economic growth. Barranquilla currently does not have historical records that can enable the identification of the relationship between air pollutant emissions and the city's

air quality, so this study provided this information so that the authorities can develop pollution-mitigation measures and prevent the adverse atmospheric and health impacts of particulate matter. However, there is still a need to complement the chemical characterization of atmospheric particulate matter and establish action plans that can minimize the impacts on human health and the environment. Future works should attempt to assess the contribution of meteorological variables on the overall interaction between urban levels and air pollutant concentrations. Another major caveat of the current study is related to the limited number of monitoring stations considered. While the obtained results are meaningful with practical significance for Barranquilla city, it is still worth noting that Barranquilla is a large area and the monitoring stations considered represent only a small zone.

Acknowledgment

The authors gratefully acknowledge financial support from the Departamento Administrativo de Ciencia, Tecnología e Innovación (Colciencias) for Project #141180764164, Contract 213-2018. Special thanks to James C. Hower of University of Kentucky, US.

References

Agudelo-Castañeda, D.M., Teixeira, E.C., Schneider, I., Pereira, F.N., Oliveira, M.L.S., Taffarel, S.R., Sehn, J.L., Ramos, C.G., Silva, L.F.O., 2016. Potential utilization for the evaluation of particulate and gaseous pollutants at an urban site near a major highway. *Sci. Total Environ.* 543(A), 161–170. <https://doi.org/10.1016/j.scitotenv.2015.11.030>.

- Alcaldía de Barranquilla, 2020. Conoce a Barranquilla.
<https://www.barranquilla.gov.co/descubre/conoce-a-barranquilla>
- Aldabe, J., Elustondo, D., Santamaría, C., Lasheras, E., Pandolfi, M., Alastuey, A., Querol, X., Santamaría, J.M., 2011. Chemical characterisation and source apportionment of PM_{2.5} and PM₁₀ at rural, urban and traffic sites in Navarra (North of Spain). *Atmos. Res.* 102(1–2), 191–205. <https://doi.org/10.1016/j.atmosres.2011.07.003>.
- Amato, F., Favez, O., Pandolfi, M., Alastuey, A., Querol, X., Moukhtar, S., Bruge, B., Verlhac, S., Orza, J.A.G., Bonnaire, N., Le Priol, T., Petit, J.F., Sciare, J., 2016. Traffic induced particle resuspension in Paris: Emission factors and source contributions. *Atmos. Environ.* 129, 114–124. <https://doi.org/10.1016/j.atmosenv.2016.01.022>.
- Arana, A., Artaxo, P., 2014. Elementary composition of atmospheric aerosol in the central region of the Amazon basin. *Quim. Nova.* 37(2), 268–276. <https://doi.org/10.5935/0100-4042.20140046>.
- Archanjo, B.S., Araujo, J.R., Silva, A.M., Capaz, R.B., Falcão, N.P.S., Jorio, A., Achete, C.A., 2014. Chemical analysis and molecular models for calcium-oxygen-carbon interactions in black carbon found in fertile Amazonian anthrosoils. *Environ. Sci. Technol.* 48(13), 7445–7452. <https://doi.org/10.1021/es501046b>.
- Arick, D.Q., Choi, Y.H., Kim, H.C., Won, Y.Y., 2015. Effects of nanoparticles on the mechanical functioning of the lung. *Adv. Colloid Interf. Advances in Colloid & Interface* 225, 218–228.
- Argumedo, C.D., Castillo, J.F., 2016. Chemical characterization of particulated atmospheric matter PM₁₀ in Guajira, Colombia. *Rev. Colomb. Quim.* 45(2), 19–29. <https://doi.org/10.15446/rev.colomb.quim.v45n2.56991>.

- Badillo-Castañeda, C.T., Garza-Ocañas, L., Garza-Ulloa, M.H., Zanatta-Calderón, M.T., Caballero-Quintero, A., 2015. Heavy metal content in PM_{2.5} air samples collected in the Metropolitan Area of Monterrey, México. *Hum. Ecol. Risk Assess.* 21 (8), 2022–2035.
- Bhuyan, P., Deka, P., Prakash, A., Balachandran, S., Hoque, R.R., 2018. Chemical characterization and source apportionment of aerosol over mid Brahmaputra Valley, India. *Environ. Pollut.* 234, 997–1010. <https://doi.org/10.1016/j.envpol.2017.12.009>.
- Blanco-Becerra, L.C., Gáfarro-Rojas, A.I., Rojas-Roa, N.Y., 2015. Influence of precipitation scavenging on the PM_{2.5}/PM₁₀ ratio at the Kennedy locality of Bogotá, Colombia. *Rev. Fac. Ing.* 76, 58–65. <https://doi.org/10.17533/udea.ingen.n76a07>.
- Bourdrel, T., Bind, M.A., Béjot, Y., Morel, O., Arsach, J.F., 2017. Cardiovascular effects of air pollution. *Arch. Cardiovasc. Dis.* 110 (11), 634–642.
- Brito, J., Rizzo, L.V., Herckes, P., Vasconcellos, P.C., Caumo, S.E.S., Fornaro, A., Ynoue, R.Y., Artaxo, P., Andrade, M.F., 2013. Physical–chemical characterisation of the particulate matter inside two road tunnels in the São Paulo Metropolitan Area. *Atmos. Chem. Phys.* 13(24), 12199–12213. <https://doi.org/10.5194/acp-13-12199-2013>.
- Cáceres, J.O., Sanz-Mangas, D., Manzoor, S., Pérez-Arribas, L.V., Anzano, J., 2019. Quantification of particulate matter, tracking the origin and relationship between elements for the environmental monitoring of the Antarctic region. *Sci. Total Environ.* 665, 125–132. <https://doi.org/10.1016/j.scitotenv.2019.02.116>.
- Canales-Rodríguez, M.A., Quintero-Núñez, M., Castro-Romero, T.G., García-Cuento, R.O., 2014. Chemical Composition of Inhalable Particles PM₁₀ in the Urban and Rural Area of Mexicali, Baja California in México. *Inf. Tecnol.* 25(6), 13–22. <https://doi.org/10.4067/S0718-07642014000600003>.

- Castillo-Ramírez, M.C., Berdejo, J., Saltaín, M., 2018. Informe anual de Calidad de Aire de Barranquilla (in Spanish). <http://barranquillaverde.gov.co/calidad-del-aire>
- Cereceda-Balic F., Toledo M., Vidal V., Guerrero F., Diaz-Robles L.A., Petit-Breuilh X., Lapuerta M., 2017. Emission factors for PM_{2.5}, CO, CO₂, NO_x, SO₂ and particle size distributions from the combustion of wood species using a new controlled combustion chamber 3CE. *Sci. Total Environ.* 584, 901-910.
- Cesari, D., De Benedetto, G.E., Bonasoni, P., Busetto, M., Dinelli A., Merico, E., Chirizzi, D., Cristofanelli, P., Donato, A., Grasso, F.M., Marinoni A., Pennetta, A., Contini, D., 2018. Seasonal variability of PM_{2.5} and PM₁₀ composition and sources in an urban background site in Southern Italy. *Sci. Total Environ.* 612, 202–213. <https://doi.org/10.1016/j.scitotenv.2017.08.239>.
- Chen, C., Liu, S., Dong, W., Zhao, B., Deng, F., 2021. Increasing cardiopulmonary effects of ultrafine particles at relatively low fine particle concentrations. *Science of the Total Environment* 751,141726.
- Cheung, K.L., Ntziachristos, L., Tzankiozis, T., Schauer, J.J., Samaras, Z., Moore, K.F., Sioutas, C., 2010. Emissions of particulate trace elements, metals and organic species from gasoline, diesel, and biodiesel passenger vehicles and their relation to oxidative potential. *Aerosol Sci. Tech.* 44(7), 500–513. <https://doi.org/10.1080/02786821003758294>.
- CIOH - Centro de Investigaciones Oceanográficas e Hidrográficas, 2007. Climatología de los principales puertos del Caribe Colombiano – Barranquilla (in Spanish). https://www.cioh.org.co/derrotero/images/PDFExternos/Climatologia_Barranquilla.pdf
- Cui, X.X., Li, F., Xiang, J.B., Fang, L., Chung, M.K., Day, D.B., Mo, J.H., Weschler, C.J., Gong, J.C., He, L.C., Zhu, D., Lu, C.J., Han, H.L., Zhang, Y.P., Zhang, J.F., 2018.

- Cardiopulmonary effects of overnight indoor air filtration in healthy non-smoking adults: a double-blind randomized crossover study. *Environ. Int.* 114, 27-36,
- Contini, D., Cesari, D., Conte, M., Donato, A., 2016. Application of PMF and CMB receptor models for the evaluation of the contribution of a large coal-fired power plant to PM_{10} concentrations. *Sci. Total Environ.* 560–561, 131–140. <https://doi.org/10.1016/j.scitotenv.2016.04.031>.
- Contini, D., Genga, A., Cesari, D., Siciliano, M., Donato, A., Ecce, M.C., Guascito, M.R., 2010. Characterisation and source apportionment of PM_{10} in an urban background site in Lecce. *Atmos. Res.* 95(1), 40–54. <https://doi.org/10.1016/j.atmosres.2009.07.010>.
- Delicado, P., 2008. Curso de Modelos Não Paramétricos. http://www-eio.upc.es/~delicado/docencia/Apuntes_Modelos_No_Parametrics.pdf (in Portuguese)
- Duarte, A.L., DaBoit, K., Oliveira, M.L.S., Teixeira, E.C., Schneider, I.L., Silva, L.F.O., 2019. Hazardous elements and amorphous nanoparticles in historical estuary coal mining area. *Geoscience Frontier* 10, 927-939.
- Farahmandkia, Z., Moattar, F., Zayeri, F., Sekhavatjou, M.S., Mansouri, N., 2017. Contribution of point and small-scaled sources to the PM_{10} emission using positive matrix factorization model. *J. Environ. Health Sci. Engineer.* 15, 2. <https://doi.org/10.1186/s40201-016-0265-8>.
- Gao, J., Peng, X., Chen, G., Xu, J., Shi, G.L., Zhang, Y.C., Feng, Y.C., 2016. Insights into the chemical characterization and sources of $PM_{2.5}$ in Beijing at a 1-h time resolution. *Sci. Total Environ.* 542(A), 162–171. <https://doi.org/10.1016/j.scitotenv.2015.10.082>.
- Gautam, S., Patra, A.K., Sahu, S.P., Hitch, M., 2018. Particulate matter pollution in opencast coal mining areas: a threat to human health and environment. *Int. J. Min. Reclam. Env.* 32(2), 75–92. <https://doi.org/10.1080/17480930.2016.1218110>.

- Gu, J., Du, S., Han, D., Hou, L., Yi, J., Xu, J., Liu, G., Han, B., Yang, G., Bai, Z.P., 2014. Major chemical compositions, possible sources, and mass closure analysis of PM_{2.5} in Jinan, China. *Air Qual. Atmos. Health* 7, 251–262. <https://doi.org/10.1007/s11869-013-0232-9>.
- Hao, Y., Meng, X., Yu, X., Lei, M., Li, W., Shi, F., Yang, W., Zhang, S., Xie, S., 2018. Characteristics of trace elements in PM_{2.5} and PM₁₀ of Chifeng, northeast China: Insights into spatiotemporal variations and sources. *Atmos. Res.* 213, 550–561. <https://doi.org/10.1016/j.atmosres.2018.07.006>.
- Hopke, P.K., 2003. A guide to Positive Matrix Factorization. <http://www.epa.gov/ttnamti1/files/ambient/pm25/workshop/laymen.pdf>
- IDEAM - Instituto de Hidrología, Meteorología y Estudios Ambientales, 2018. Informe del Estado de la Calidad del Aire en Colombia 2017 (in Spanish). <http://www.ideam.gov.co/web/concentracion-y-calidad-ambiental/informes-del-estado-de-la-calidad-del-aire-en-colombia>
- Jain, S., Sharma, S.K., Mandel, T.K., Saxena, M., 2018. Source apportionment of PM₁₀ in Delhi, India using PCA/APCS, UNMIX and PMF. *Particuology* 37, 107–118. <https://doi.org/10.1016/j.partic.2017.05.009>.
- Jaiprakash, H. G., 2017. Chemical and optical properties of PM_{2.5} from on-road operation of light duty vehicles in Delhi city. *Sci. Total Environ.* 586, 900–916. <https://doi.org/10.1016/j.scitotenv.2017.02.070>.
- Kholod, N., Evans, M., 2016. Reducing black carbon emissions from diesel vehicles in Russia: An assessment and policy recommendations. *Environ. Sci. Policy.* 56, 1–8. <https://doi.org/10.1016/j.envsci.2015.10.017>.

- Kubesch, N.J., Nazelle, A. de, Westerdahl, D., Martinez, D., Carrasco-Turigas, G., Bouso, L., Guerra, S., Nieuwenhuijsen, M.J., 2015. Respiratory and inflammatory responses to short-term exposure to traffic-related air pollution with and without moderate physical activity. *Occup. Environ. Med.* 72, 284-293.
- Kumar, R., Chauhan, M., Sharma, N., Chaudhary, G.R., 2018. Toxic effects of nanomaterials on environment. *Environmental Toxicity of Nanomaterials*, CRC Press, 1-20.
- Li, T.C., Yuan, C.S., Huang, H.C., Lee, C.L., Wu, S.P., Tong, C., 2016. Inter-comparison of Seasonal Variation, Chemical Characteristics, and Source Identification of Atmospheric Fine Particles on Both Sides of the Taiwan Strait. *Sci. Rep.* 6, 22956. <https://doi.org/10.1038/srep22956>.
- Liu, Y., Xing, J., Wang, S., Fu, X., Zhang, H., 2018. Source-specific speciation profiles of PM_{2.5} for heavy metals and their anthropogenic emissions in China. *Environ. Pollut.* 239, 544–553. <https://doi.org/10.1016/j.envpol.2018.04.047>.
- Liu, B., Song, N., Dai, Q., Mei, K., Sui, B., Bi, X., Feng, Y., 2016. Chemical composition and source apportionment of ambient PM_{2.5} during the non-heating period in Taian, China. *Atmos. Res.* 170, 23–33. <https://doi.org/10.1016/j.atmosres.2015.11.002>.
- López, M.L., Ceppi, S., Palancar, G.G., Olcese, L.E., Tirao, G., Toselli, B.M., 2011. Elemental concentration and source identification of PM₁₀ and PM_{2.5} by SR-XRF in Córdoba City, Argentina. *Atmos. Environ.* 45(31), 5450–5457. <https://doi.org/10.1016/j.atmosenv.2011.07.003>.
- Maldonado-Arízaga, M.J., 2012. Caracterización del material particulado suspendido PM₁₀ de la red de monitoreo de aire de la ciudad de Quito de los años 2009 y 2010 por

- Espectroscopía de Absorción Atómica (in Spanish).
<http://repositorio.puce.edu.ec/handle/22000/7112>.
- Morera-Gómez, Y., Elustondo, D., Lasheras, E., Alonso-Hernández, C. M., Santamaría, J.M., 2018. Chemical characterization of PM₁₀ samples collected simultaneously at a rural and an urban site in the Caribbean coast: Local and long-range source apportionment. *Atmos. Environ.* 192, 182–192.
<https://doi.org/10.1016/j.atmosenv.2018.08.058>.
- Mugica, V., Ortiz, E., Molina, L., De Vizcaya-Ruiz, A., Nebot, A., Quintana, R., Aguilar, J., Alcántara, E., 2009. PM composition and source reconciliation in Mexico City. *Atmos. Environ.* 43(32), 5068–5074. <https://doi.org/10.1016/j.atmosenv.2009.06.051>.
- Murillo, J.H., Roman, S.R., Marin, J.F.R., Ramos, A.C., Jimenez, S. B., Gonzalez, B.C., Baumgardner, D.G., 2013. Chemical characterization and source apportionment of PM₁₀ and PM_{2.5} in the metropolitan area of Costa Rica, Central America. *Atmos. Pollut. Res.* 4(2), 181–190. <https://doi.org/10.1016/APR.2013.018>.
- Ordóñez-Aquino, C., Sánchez-Ccoyllo, O., 2017. Characterization of the PM_{2.5} chemical - morphological in Lima metropolitan with scanning electronic microscopy (SEM). *Rev. Acta. Nova.* 8(3), 397–420.
- Paatero, P., Tapper, U., 1994. Positive matrix factorization: a non-negative factor model with optimal utilization of error estimates of data values. *Environmetrics* 5, 111–126.
<https://doi.org/10.1002/env.3170050203>.
- Palomino, G., 2016. Motores lineales de imanes permanentes: Principios de funcionamiento y optimización, Programa Editorial Universidad Autónoma de Occidente, Santiago de Cali.(in Spanish),

- Park, M., Joo, H.S., Lee, K., Jang, M., Kim, S.D., Kim, I., Borlaza, L.J.S., Lim, H., Shin, H., Chung, K.H., Choi, Y.H., Park, S.G., Bae, M.S., Lee, J., Song, H., Park, K., 2018. Differential toxicities of fine particulate matters from various sources. *Sci. Rep.* 8, 17007. <https://doi.org/10.1038/s41598-018-35398-0>.
- Peters, A., Hampel, R., Cyrys, J., Breitner, S., Geruschkat, U., Kraus, U., Zareba, W., Schneider, A., 2015. Elevated particle number concentrations induce immediate changes in heart rate variability: a panel study in individuals with impaired glucose metabolism or diabetes. *Part. Fibre. Toxicol.* 12, 7.
- Perrone, M.G., Vratolis, S., Georgieva, E., Török, S., Šeĉa, K., Veleva, B., Osán, J., Bešlić, I., Kertész, Z., Pernigotti, D., Eleftheriadis, K., Belis, C.A., 2018. Sources and geographic origin of particulate matter in urban areas of the Danube macro-region: The cases of Zagreb (Croatia), Budapest (Hungary) and Sofia (Bulgaria). *Sci. Total Environ.* 619–620, 1515–1529. <https://doi.org/10.1016/j.scitotenv.2017.11.092>.
- Pillai, P.S., Babu, S.S., Moorthy, K.K., 2002. A study of PM, PM₁₀ and PM_{2.5} concentration at a tropical coastal station. *Atmos. Res.* 61(2), 149–167. [https://doi.org/10.1016/S0169-8095\(01\)00136-3](https://doi.org/10.1016/S0169-8095(01)00136-3).
- Police, S., Sahu, S.K., Tiwari, M., Pandit, G.G., 2018. Chemical composition and source apportionment of PM_{2.5} and PM_{2.5–10} in Trombay (Mumbai, India), a coastal industrial area. *Particuology.* 37, 143–153. <https://doi.org/10.1016/j.partic.2017.09.006>.
- Putaud, J.P., Van Dingenen, R., Alastuey, A., Bauer, H., Birmili, W., Cyrys, J., Flentje, H., Fuzzi, S., Gehrig, R., Hansson, H.C., Harrison, R.M., Herrmann, H., Hitztenberger, R., Hüglin, C., Jones, A.M., Kasper-Giebl, A., Kiss, G., Kousa, A., Kuhlbusch, T.A.J., Löschau, G., Maenhaut, W., Molnar, A., Moreno, R., Pekkanen, J., Perrino, C., Pitz, M., Puxbaum, H., Querol, X., Rodriguez, S., Salma, I., Schwarz, J., Smolik, J., Schneider, J.,

- Spindler, G., ten Brink, H., Tursoc, J., Viana, M., Wiedensohler, A., Raes, F., 2010. A European aerosol phenomenology - 3: Physical and chemical characteristics of particulate matter from 60 rural, urban, and kerbside sites across Europe. *Atmos. Environ.* 44(10), 1308–1320. <https://doi.org/10.1016/j.atmosenv.2009.12.011>.
- Querol, X., Alastuey, A., de la Rosa, J., Sánchez de la Campa, A., Plana, F., Ruiz, C.R., 2002. Source apportionment analysis of atmospheric particulates in an industrialised urban site in southwestern Spain. *Atmos. Environ.* 36(19), 3113–3125. [https://doi.org/10.1016/S1352-2310\(02\)00257-1](https://doi.org/10.1016/S1352-2310(02)00257-1).
- Querol, X., Alastuey, A., Rodriguez, S., Plana, F., Ruiz, C.R., Cots, N., Massagué, G., Puig, O., 2001. PM₁₀ and PM_{2.5} source apportionment in the Barcelona Metropolitan area, Catalonia, Spain. *Atmos. Environ.* 35(36), 6407–6419. [https://doi.org/10.1016/S1352-2310\(01\)00361-2](https://doi.org/10.1016/S1352-2310(01)00361-2).
- Ramírez, O., Sánchez de la Campa, A.M., Amato, F., Catacolí, R.A., Rojas, N., de la Rosa, J., 2018a. Chemical composition and source apportionment of PM₁₀ at an urban background site in a high-altitude Latin American megacity (Bogota, Colombia). *Environ. Pollut.* 233, 142–155. <https://doi.org/10.1016/j.envpol.2017.10.045>.
- Reff, A., Eberly, S.I., Phave, P. V., 2007. Receptor modeling of ambient particulate matter data using Positive Matrix Factorization: review of existing methods. *J. Air Waste Manage.* 57(2), 146–154. <https://doi.org/10.1080/10473289.2007.10465319>.
- Riojas-Rodríguez, H., da Silva, A.S., Texcalac-Sangrador, J.L., Moreno-Banda, G.L., 2016. Air pollution management and control in Latin America and the Caribbean: implications for climate change. *Rev. Panam. Salud Publica* 40(3), 150–159. <https://www.scielosp.org/article/rpsp/2016.v40n3/150-159/en/>.

- Rojano, R., Arregoces, H., Restrepo, G., 2014. Elemental Composition and Sources of Inhalable Particles (PM₁₀) and Suspended Total Particles (TSP) in the Urban Area of the City of Riohacha' Colombia. *Inf. Tecnol.* 25(6), 3–12. <https://doi.org/10.4067/S0718-07642014000600002>.
- Saldarriaga-Molina, J.C., Echeverri-Londoño, C.A., Molina-Pérez, F.J., 2004. Partículas suspendidas (PST) y partículas respirables (PM₁₀) en el Valle de Aburrá, Colombia. *Rev. Fac. Ing. Univ. Antioquia.* 32, 7–16 (in Spanish). <https://www.redalyc.org/articulo.oa?id=430/43003201>.
- Salvador, P., Artíñano, B., Querol, X., Alastuey, A., Coscío, M., 2007. Characterisation of local and external contributions of atmospheric particulate matter at a background coastal site. *Atmos. Environ.* 41(1), 1–17. <https://doi.org/10.1016/j.atmosenv.2006.08.007>.
- Salvo, A., Brito, J., Artaxo, P., Geiger, F.M., 2017. Reduced ultrafine particle levels in São Paulo's atmosphere during shift from gasoline to ethanol use. *Nat. Commun.* 8, 77. <https://doi.org/10.1038/s41467-017-00041-5>.
- Santos Junior, D.A.M., 2015. Emissões veiculares em São Paulo: Quantificação de fontes com modelos receptores e caracterização do material carbonáceo. São Paulo: Instituto de Física, Universidade de São Paulo, 2015. Dissertação de Mestrado em Física.(in Portuguese) <https://doi.org/10.11606/D.43.2015.tde-17072015-135624>.
- Saraga, D.E., Tolis, E.I., Maggos, T., Vasilakos, C., Bartzis, J.G., 2019. PM_{2.5} source apportionment for the port city of Thessaloniki, Greece. *Sci. Total Environ.* 650(2), 2337–2354. <https://doi.org/10.1016/j.scitotenv.2018.09.250>.

- Scerri, M.M., Kandler, K., Weinbruch, S., 2016. Disentangling the contribution of Saharan dust and marine aerosol to PM₁₀ levels in the Central Mediterranean. *Atmos. Environ.* 147, 395–408. <https://doi.org/10.1016/j.atmosenv.2016.10.028>.
- Schneider, I.L., Teixeira, E.C., Oliveira, L.F.S., Wiegand, F., 2015. Atmospheric particle number concentration and size distribution in a traffic-impacted area. *Atmos. Pollut. Res.* 6(5), 877–885. <https://doi.org/10.5094/APR.2015.097>.
- Silva, L.F.O., Milanes, C., Pinto, D., Ramirez, O., Lima, B.D., 2020a. Multiple hazardous elements in nanoparticulate matter from a Caribbean industrialized atmosphere. *Chemosphere* 239, 124776.
- Silva, L.F.O., Pinto, D., Neckel, A., Oliveira, M.L.S., Sampaio, C.H., 2020b. Atmospheric nanocompounds on Lanzarote Island: Vehicular exhaust and igneous geologic formation interactions. *Chemosphere* 254, 126922.
- Soleimani, M., Amini, N., Sadeghian, B., Wang, D., Fang, L., 2018. Heavy metals and their source identification in particulate matter (PM_{2.5}) in Isfahan City, Iran. *J. Environ. Sci.* 72, 166–175. <https://doi.org/10.1016/j.jes.2018.01.002>.
- Song, X., Yang, S., Shao, Y., Fan, J., Liu, Y., 2016. PM₁₀ mass concentration, chemical composition, and sources in the typical coal-dominated industrial city of Pingdingshan, China. *Sci. Total Environ.* 571, 1155–1163. <https://doi.org/10.1016/j.scitotenv.2016.07.115>.
- Souza, I.C., Mendes, V.A.S., Duarte, I.D., Rocha, L.D., Azevedo, V.C., Matsumoto, S.T., Elliott, M., Wunderlin, D.A., Monferrán, M.V., Fernandes, M.N., 2019. Nanoparticle transport and sequestration: intracellular titanium dioxide nanoparticles in a neotropical fish. *Sci. Total Environ.* 658, 798-808.

- Taiwo, A.M., 2016. Source apportionment of urban background particulate matter in Birmingham, United Kingdom using a mass closure model. *Aerosol and Air Qual. Res.* 16(5), 1244–1252. <https://doi.org/10.4209/aaqr.2015.09.0537>.
- Tao, J., Gao, J., Zhang, L., Zhang, R., Che, H., Zhang, Z., Lin, Z., Jing, J., Cao, J., Hsu, S.C., 2014. PM_{2.5} pollution in a megacity of Southwest China: Source apportionment and implication. *Atmos. Chem. Phys.* 14(16), 8679–8699. <https://doi.org/10.5194/acp-14-8679-2014>.
- Tasić, M., Mijić, Z., Rajšić, S., Stojić, A., Radenković, M., Joksić, J., 2009. Source apportionment of atmospheric bulk deposition in the Belgrade urban area using Positive Matrix factorization. *J. Phys.: Conf. Se.* 162, 012018. <https://doi.org/10.1088/1742-6596/162/1/012018>.
- Terzi, E., Argyropoulos, G., Bougatiot, A., Mihalopoulos, N., Nikolaou, K., Samara, C., 2010. Chemical composition and mass closure of ambient PM₁₀ at urban sites. *Atmos. Environ.* 44(18), 2231–2239. <http://doi.org/10.1016/j.atmosenv.2010.02.019>.
- Tiwary A., Williams I., 2018. *Air Pollution: Measurement, Modelling and Mitigation*. CRC Press, 696 pp.
- Tsyro, S.G., 2005. To what extent can aerosol water explain the discrepancy between model calculated and gravimetric PM₁₀ and PM_{2.5}? *Atmos. Chem. Phys.* 5(2), 515–532. <https://doi.org/10.5194/acp-5-515-2005>.
- Tomasi, C., Fuzzi, S., Kokhanovsky, A., 2017. Atmospheric Aerosols: Life Cycles and Effects on Air Quality and Climate. *Remote Sensing of Atmospheric Aerosol*, 341-436.
- USEPA – United States Environmental Protection Agency, 2014. EPA Positive Matrix Factorization (PMF) 5.0 Fundamentals and User Guide – EPA/600/R-14/108. https://www.epa.gov/sites/production/files/2015-02/documents/pmf_5.0_user_guide.pdf

- Vallius, M., Lanki, T., Tiittanen, P., Koistinen, K., Ruuskanen, J., Pekkanen, J., 2003. Source apportionment of urban ambient PM_{2.5} in two successive measurement campaigns in Helsinki, Finland. *Atmos. Environ.* 37(5), 615–623. [https://doi.org/10.1016/S1352-2310\(02\)00925-1](https://doi.org/10.1016/S1352-2310(02)00925-1).
- Vargas, F.A., Rojas, N.Y., Pachon, J.E., Russell, A.G., 2011. PM₁₀ characterization and source apportionment at two residential areas in Bogota. *Atmos. Pollut. Res.* 3(1), 72–80. <https://doi.org/10.5094/APR.2012.006>.
- Vélez-Pereira, A.M., Vergara-Vasquez, E., 2013. Caracterización de emisiones atmosféricas por fuentes fijas industriales del distrito de Barranquilla, Colombia. In: 4th Colombian Meeting and International Conference on Air Quality and Public Health 1176–1183. <https://doi.org/10.13140/RG.2.1.1941.1047>.
- Vengoechea, A.M., Rojano, R.E., Arreola-Aguayo, H.A., 2018. Dispersion and Concentration of PM₁₀ Particles in a Caribbean Coastal City. *Inf. Tecnol.* 29(6), 123–130. <https://doi.org/10.4067/s0718-07042018000600123>.
- Viana, M., Querol, X., Alastuey, A., Gil, J.I., Menéndez, M., 2006. Identification of PM sources by principal component analysis (PCA) coupled with wind direction data. *Chemosphere* 65(11), 2411–2418. <https://doi.org/10.1016/j.chemosphere.2006.04.060>.
- Wang, W., Yu, J., Cui, Y., He, J., Xue, P., Cao, W., Ying, H., Gao, W., Yan, Y., Hu, B., Xin, J., Wang, L., Liu, Z., Sun, Y., Dongsheng, J., Wang, Y., 2018. Characteristics of fine particulate matter and its sources in an industrialized coastal city, Ningbo, Yangtze River Delta, China. *Atmos. Res.* 203, 105–117. <https://doi.org/10.1016/j.atmosres.2017.11.033>.

- Wang, Y., Zhuang, G., Sun, Y., An, Z., 2006. The variation of characteristics and formation mechanisms of aerosols in dust, haze, and clear days in Beijing. *Atmos. Environ.* 40(34), 6579–6591. <https://doi.org/10.1016/j.atmosenv.2006.05.066>.
- Weichenthal, S., Hatzopoulou, M., Goldberg, M.S., 2014. Exposure to traffic-related air pollution during physical activity and acute changes in blood pressure, autonomic and micro-vascular function in women: a cross-over study. *Part. Fibre. Toxicol.* 11, 70.
- WHO – World Health Organization, 2005. Air quality guidelines - global update 2005. https://www.who.int/phe/health_topics/outdoorair/outdoorair_aqg/en/.
- WHO – World Health Organization, 2018. Ambient (outdoor) air pollution. [https://www.who.int/es/news-room/fact-sheets/detail/ambient-\(outdoor\)-air-quality-and-health](https://www.who.int/es/news-room/fact-sheets/detail/ambient-(outdoor)-air-quality-and-health)
- Wu, X., Vu, T.V., Shi, Z., Harrison, P.M., Liu, D., Cen, K., 2018. Characterization and source apportionment of carbonaceous PM_{2.5} particles in China - A review. *Atmos. Environ.* 189, 187–212. <https://doi.org/10.1016/j.atmosenv.2018.06.025>.
- Xue, F., Kikumoto, H., Li, X., Ooka, R., 2018. Bayesian source term estimation of atmospheric releases in urban areas using LES approach. *J. Hazard. Mater.* 349, 68–78. <https://doi.org/10.1016/j.jhazmat.2018.01.050>.
- Yan, S., Subramanian, S.B., Tyagi, R.D., Surampalli, R.Y., Zhang, T.C., 2010. Emerging contaminants of environmental concern: source, transport, fate, and treatment. *Pract. Period. Hazard Toxic Radioact. Waste Manag.* 14 (1), 2-20.
- Yao, L., Yang, L., Yuan, Q., Yan, C., Dong, C., Meng, C., Sui, X., Yang, F., Lu, Y., Wang, W., 2016. Sources apportionment of PM_{2.5} in a background site in the North China Plain. *Sci. Total Environ.* 541, 590–598. <https://doi.org/10.1016/j.scitotenv.2015.09.123>.

- Zhong, Z., Zheng, J., Zhu, M., Huang, Z., Zhang, Z., Jia, G., Wang, X., Bian, Y., Wang, Y., Li, N., 2018. Recent developments of anthropogenic air pollutant emission inventories in Guangdong province, China. *Sci. Total Environ.* 627, 1080–1092. <https://doi.org/10.1016/j.scitotenv.2018.01.268>.
- Zhou, W., Wang, Q., Zhao, X., Xu, W., Chen, C., Du, W., Zhao, J., Canonaco, F., Prévôt, A.S.H., Fu, P., Wang, Z., Worsnop, D.R., Sun, Y., 2018. Characterization and source apportionment of organic aerosol at 260 m on a meteorological tower in Beijing, China. *Atmos. Chem. Phys.* 18(6), 3951–3968. <https://doi.org/10.5194/acp-18-3951-2018>.

LIST OF FIGURES

Figure 1. Selected study area.

Figure 2. Wind Rose for the period between April-October 2018.

Figure 3. Average $PM_{2.5}$ and PM_{10} mass concentrations in the city of Barranquilla between April–October 2018.

Figure 4. Mass closure of particulate matter (PM_{10} y $PM_{2.5}$).

Figure 5. Source profiles identified for the $PM_{2.5}$ mass samples of each species assigned to the factor (blue bar, left axis) and the percentage of each species associated with the factor (red square, right axis).

Figure 6. Source profiles identified for the PM_{10} mass samples of each species assigned to the factor (blue bar, left axis) and the percentage of each species associated with the factor (red square, right axis).

Figure 7. Source apportionment to $PM_{2.5}$ and PM_{10} mass concentrations ($\mu g/m^3$).

LIST OF TABLES

Table 1. Average concentrations ($\mu\text{g}/\text{m}^3$), standard deviation, maximum and minimum for $\text{PM}_{2.5}$ and PM_{10} , and the associated chemical elements.

Table 2. Comparison of the concentrations of PM and chemical elements ($\mu\text{g}/\text{m}^3$) obtained in this study with other investigations.

Table 3. Spearman's correlation matrix between the PM concentrations and meteorological variables. The correlations in red correspond to PM_{10} and those in black to $\text{PM}_{2.5}$.

Table 1. Average concentrations ($\mu\text{g}/\text{m}^3$), standard deviation, maximum and minimum for $\text{PM}_{2.5}$ and PM_{10} , and the associated chemical elements.

ELEMENT	PM _{2.5}		PM ₁₀				(PM _{2.5} /PM ₁₀) × 100%		
	Average	Std.Dev	Min	Max	Average	Std.Dev	Min	Max	
PM	12.01	3.19	4.27	20.13	46.67	16.25	13.36	109.25	26%
BC	1.136	0.592	0.293	3.168	2.132	1.124	0.342	5.881	53%
Mg	0.208	0.097	0.017	0.530	0.377	0.218	0.018	0.945	55%
Al	0.370	0.342	0.029	2.110	0.930	0.607	0.212	2.842	40%
Si	0.584	0.508	0.056	3.143	1.582	0.977	0.372	4.731	37%
P	0.078	0.015	0.036	0.130	0.135	0.022	0.078	0.196	58%
S	0.811	0.175	0.328	1.335	0.939	0.128	0.389	1.485	86%
Cl	0.737	0.595	0.001	2.165	4.028	1.952	0.392	8.298	18%
K	0.157	0.059	0.048	0.410	0.423	0.134	0.136	0.823	37%
Ca	0.180	0.064	0.048	0.397	1.701	0.471	0.811	3.082	11%
Ti	0.023	0.021	0.002	0.140	0.084	0.053	0.015	0.243	27%
Cr					0.205	0.001	0.002	0.008	
V	0.004	0.001	0.001	0.007	0.001	0.000	0.001	0.003	77%
Mn	0.004	0.003	0.001	0.013	0.018	0.009	0.003	0.050	24%
Fe	0.199	0.162	0.031	1.053	0.816	0.475	0.167	2.722	24%
Ni	0.001	0.004	0.001	0.035	0.002	0.004	0.001	0.040	75%
Cu	0.003	0.001	0.001	0.006	0.006	0.001	0.003	0.009	47%
Zn	0.011	0.008	0.007	0.041	0.021	0.010	0.008	0.059	53%
Pb	0.007	0.010	0.003	0.076	0.011	0.010	0.005	0.082	64%
Na ⁺	0.891	0.437	0.333	1.748					
K ⁺	0.112	0.047	0.014	0.258					
Mg ²⁺	0.100	0.047	0.003	0.200					
Ca ²⁺	0.159	0.110	0.012	0.600					
Cl ⁻	0.549	0.409	0.001	1.467					
NO ₃ ⁻	0.509	0.545	0.131	4.000					
SO ₄ ²⁻	1.392	0.405	0.121	2.882					

Table 2. Comparison of the concentrations of PM and chemical elements ($\mu\text{g}/\text{m}^3$) obtained in this study with other investigations.

Element	This study	Taiwan, China ^a	Cordoba, Argentina ^b		Belen, Costa Rica ^c	Guangzhou, China ^d	Barcelona, Spain ^e	Mexico City, Mexico ^f	Galicia, Spain ^g	Navi Mumbai, India ^h
			Site 1	Site 2						
PM _{2.5}	12.01	34.00	70.87	66.99	36	103.35	35	56	13.467	42
PM ₁₀	46.67	52.40	106.71	101.09	52	144.52	119.10	95	18.877	71
(PM _{2.5} /PM ₁₀) × 100%	26%	65%	66%	66%	69%	72%	29%	58%	71%	59%
BC _{PM2.5}	1.14	-	-	-	-	-	-	-	-	-
BC _{PM10}	2.13	-	-	-	-	-	-	-	-	-
Mg _{PM2.5}	0.21	0.32	-	-	0.15	0.31	0.08	0.3	0.14	0.22
Al _{PM2.5}	0.37	1.01	0.02	0.00	0.35	1.71	-	1.2	-	0.45
Si _{PM2.5}	0.58	-	4.21	3.80	4.21	-	-	1.9	0.84	-
P _{PM2.5}	0.08	-	-	-	-	-	1.03	-	0.023	0.028
S _{PM2.5}	0.81	-	0.13	0.14	-	-	-	-	1.503	-
Cl _{PM2.5}	0.74	-	-	-	-	-	0.59	-	-	0.26
K _{PM2.5}	0.16	-	0.23	0.17	0.12	2.71	0.48	-	0.37	0.28
Ca _{PM2.5}	0.18	0.89	0.23	0.29	0.23	1.44	0.51	0.7	0.222	0.31
Ti _{PM2.5}	0.02	0.02	0.01	0.02	-	0.03	0.02	0.3	0.004	0.023
V _{PM2.5}	0.00	0.01	0.01	0.01	0.00	0.07	0.009	0.02	0.015	0.0091
Mn _{PM2.5}	0.00	0.01	0.01	0.01	0.35	-	0.014	0.05	0.003	0.0092
Fe _{PM2.5}	0.20	0.17	0.33	0.35	0.21	0.03	0.26	2.7	0.063	0.31
Ni _{PM2.5}	0.00	0.01	0.00	0.00	0.01	0.03	0.006	0.03	0.004	0.0063
Cu _{PM2.5}	0.00	0.01	0.01	0.01	0.10	0.10	0.052	0.15	0.028	0.0062
Zn _{PM2.5}	0.01	0.10	0.03	0.03	-	0.86	0.178	0.60	0.017	0.064
Pb _{PM2.5}	0.01	0.02	0.00	0.00	0.01	-	0.130	0.18	0.007	0.036
Mg _{PM10}	0.38	0.51	-	-	0.15	1.05	0.29	0.4	0.153	0.68
Al _{PM10}	0.93	1.49	0.10	0.08	0.74	8.06	-	2.9	-	1.65
Si _{PM10}	1.58	-	25.95	17.80	2.00	-	-	4.9	-	4.1
P _{PM10}	0.14	-	-	-	-	-	0.04	-	0.014	0.044
S _{PM10}	0.94	-	0.29	0.28	-	-	-	-	-	0.99
Cl _{PM10}	4.03	-	-	-	-	-	1.10	-	-	2.3
K _{PM10}	0.42	-	1.93	1.70	0.23	3.38	0.56	-	0.175	0.43
Ca _{PM10}	1.70	1.07	3.88	3.93	0.37	4.29	2.25	1.5	0.134	2.4
Ti _{PM10}	0.08	0.06	0.32	0.27	-	0.14	0.05	0.3	0.007	0.17
V _{PM10}	0.01	0.01	0.02	0.02	-	0.08	0.013	0.03	0.005	0.0072
Cr _{PM10}	0.00	0.03	0.01	0.01	0.01	0.08	0.006	0.07	-	0.026
Mn _{PM10}	0.02	0.02	0.09	0.07	0.14	0.10	0.024	0.06	0.005	0.041
Fe _{PM10}	0.82	0.57	3.80	3.05	0.55	0.13	0.89	3.3	0.137	1.9
Ni _{PM10}	0.00	0.01	0.01	0.00	0.01	0.04	0.007	0.05	0.003	0.0023
Cu _{PM10}	0.01	0.02	0.03	0.01	0.15	0.02	0.074	0.18	0.008	0.019
Zn _{PM10}	0.02	0.13	0.06	0.03	-	0.90	0.25	0.64	0.016	0.084
Pb _{PM10}	0.01	0.02	0.01	0.00	0.01	-	0.149	0.33	0.008	0.024
Region	Urban	Urban	Semi Urban		Industrial	Urban	Urban	Urban	Semi Urban	Urban

Note: ^aChin et al. (2016), ^bLópez et al. (2011), ^cMurillo et al. (2013), ^dWang et al. (2006), ^eQuerol et al. (2001), ^fMugica et al. (2009), ^gSalvador et al. (2007), ^hPolice et al. (2018).

Table 3. Spearman's correlation matrix between the PM concentrations and meteorological variables. The correlations in red correspond to PM₁₀ and those in black to PM_{2.5}.

	PM _{2.5}	PM ₁₀	BC	T	RH	Rad	Precip	Atm. Pres.	WS	WD
PM _{2.5}	1	0.890**	-0.191	0.035	-0.212	0.317**	-0.206	-0.051	0.280*	-0.351**
PM ₁₀	0.890**	1	-0.318**	0.123	-0.205	0.467**	-0.316**	-0.199	0.386**	-0.343**
BC	-0.328**	-0.464**	1	0.300**	0.214	-0.474**	0.383**	0.328**	-0.468**	0.310**
T	0.035	0.123	-0.196	1	-0.413**	0.436**	-0.257*	-0.515**	-0.056	0.035
RH	-0.212	-0.205	0.274*	0.413**	1	-0.561**	0.363**	0.270*	-0.439**	0.033
Rad	0.317**	0.467**	-0.573**	0.436**	-0.561**	1	-0.474**	-0.364**	0.571**	-0.201
Precip.	-0.206	-0.316**	0.401**	-0.257*	0.363**	-0.474**	1	0.266*	-0.498**	0.149
Atm. Pres.	-0.051	-0.199	0.215	0.515**	0.270*	-0.364**	0.266*	1	-0.218*	0.029
WS	0.280*	0.386**	-0.585**	-0.056	-0.439**	0.571**	-0.498**	-0.218*	1	-0.295**
WD	-0.351**	-0.343**	0.322**	0.035	0.033	-0.201	0.149	0.029	-0.295**	1

* Correlation is significant at the 0.05 level

** Correlation is significant at the 0.01 level

The authors have not conflict of interest.

Journal Pre-proof

HIGHLIGHTS

- PM_{10} and $PM_{2.5}$ concentrations and the chemical elements associated were evaluated.
- PMF receptor model indicated five emission sources for each PM fraction.
- PM_{10} predominant sources were civil works, resuspended soil, and marine spray.
- $PM_{2.5}$ main sources were fuel oil combustion and fertilizer industry emissions.